

Performance of a Reservoir Subject to Simultaneous Two-Edged and Bottom Water Drive Mechanisms.

¹Edo, T. M and ²Adewole E. S.

¹Department of Petroleum Engineering, Edo State Institute of Technology and Management, Usen
²Department of Petroleum Engineering, University of Benin, Benin City

Abstract

The objective of this study is to analyzing the performance of a reservoir subject to simultaneous two edged and bottom water drive mechanism in terms of pressure distribution for the purpose of optimizing oil production. Source and Green's functions are utilized in deriving the dimensionless pressure expressions for reservoir with double edged and bottom water drive. It is assumed that the horizontal well is centrally located with the two edged water occurring both at the toe and at the heel of the well. Influences of reservoir and wellbore properties are investigated for infinite-acting flow and after infinite-acting flow conditions. Results show that, the period of infinite activity is extended if the reservoir is much larger than the length of the well and the wellbore radius is small. Furthermore, dimensionless time of attainment of steady state for all well design is strongly dependent on the reservoir extent and the reservoir anisotropy under constant rate regime.

1.0 Introduction

Horizontal wells are usually drilled perpendicular to maximum permeability direction to maximize recovery. Transient pressure behavior of horizontal wells has been well documented [1-5].

Reservoir permeability is one property that changes with direction, that is, the reservoir is said to be anisotropic in nature. This property tends to influence the pressure distribution in the well since the interconnected pores through which fluid flow, to create a pressure variation, is a function of permeability. This study is restricted to only permeability, as an anisotropic property, that influences pressure distribution.

Karakas *et al.*[6], investigated the transient pressure behavior of dual-lateral horizontal wells. They used a numerical simulator to predict the pressure response and analyze the field data from dual-lateral wells. Raghavan and Ambashta [7] presented a semianalytical flow model to simulate the transient flow into multilateral wells. They identified the flow regimes and proposed asymptotic solutions for each flow regime

For the first time, Gringarten and Ramey[8], constructed instantaneous source functions which can be used to derive mathematical models for fluid flow in reservoirs and well bores, for various types of reservoir boundaries. Although, the usefulness of these relationships was also demonstrated in good detail, the first application was done by Cinco *et al* [9] to generate analytic solutions for unsteady-state pressure distribution created by a directionally drilled well in an isotropic medium. For somewhat closer to a horizontal well, Raghavan *et al* [10] and Rodrigues *et al* [11] obtained analytical solution to the problem of transient flow of fluids in fully and partially penetrating fractures.

Nomenclature

h = reservoir thickness, ft

h_D = dimensionless reservoir thickness

l_D = dimensionless well length

s = source function

t_D = dimensionless time

$x, y, z,$ = distance in the $x, y, z,$ direction, ft, respectively

x_D, y_D, z_D = dimensionless distances in the $x, y,$ and z direction respectively

Corresponding author: Edo, T. M, E-mail: taiwoedo@yahoo.com, Tel.: +2348035111409

- k_x, k_y, k_z = permeability in the x, y and z direction respectively, md
- p_D = dimensionless pressure
- r_{wD} = dimensionless wellbore radius
- ϕ = reservoir porosity
- μ =oil viscosity, cp
- τ =dummy integration variable
- η =diffusivity constant, mdpsi/cp

2.0 Reservoir and Mathematical Description of Model

The following assumptions were made for the selection of this model:

- 1 The reservoir is homogenous and having constant and uniform thickness with gas cap at the top and water at the bottom and edges of the formation.
- 2 Constant porosity and varying permeability in each direction.
- 3 Gravitational and frictional effects are negligible
- 4 No-flow boundary only at the top of the reservoir.

Figure 1 shows the reservoir under study. It has a horizontal well producing oil of small and constant compressibility under a constant draw down rate pressure P_i . If reservoir well experiences a drawdown pressure of $\Delta P = P_i - P(x, y, z, t)$ for a certain time, t , it is intended to derive a generalized dimensionless pressure as a function of reservoir, well and fluid properties. The horizontal well experiences water energy (constant pressure support) from the heel and toe owing to edge water drive from the reservoir. The reservoir is anisotropic, with k_x, k_y and k_z as its permeabilities along the principal axes. Furthermore, it is seated at the toe (top) of the well and infinite laterally along the well width(y-direction). Hence, the horizontal well is a line source.

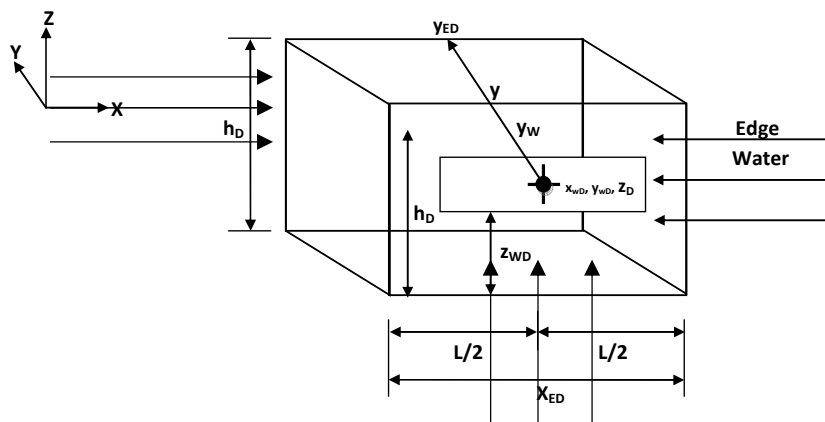


Fig. 1: Two Edged and Bottom Reservoir Model: Infinite acting period

During the infinite acting period, the pressure transients have not felt any of the external boundaries. The required source functions are: infinite slab source in an infinite slab reservoir in the x- direction, an infinite plane source in an infinite reservoir and an infinite plane source in an infinite reservoir. These sources are written as follows

X-Axis:

$$S(x,t) = \frac{1}{2} \left[\operatorname{erf} \frac{\frac{x_f}{2} + (x-x_w)}{2\sqrt{\eta_x t}} + \operatorname{erf} \frac{\frac{x_f}{2} - (x-x_w)}{2\sqrt{\eta_x t}} \right] \dots\dots\dots (1)$$

Y-Axis:

$$S(y,t) = \exp \left[-(y - y_w)^2 / 4\eta_y t \right] / 2\sqrt{\pi\eta_y t} \dots\dots\dots (2)$$

Z-Axis:

$$S(z,t) = \exp \left[-(z - z_w)^2 / 4\eta_z t \right] / 2\sqrt{\pi\eta_z t} \dots\dots\dots (3)$$

In dimensionless form equation (1) becomes

$$S(x_D, t_D) = \frac{1}{2} \left[\operatorname{erf} \frac{x_D + \sqrt{\frac{k_x}{k}}}{2\sqrt{t_D \frac{k_x}{k_h}}} + \operatorname{erf} \frac{\sqrt{\frac{k_x}{k}} - x_D}{2\sqrt{t_D \frac{k_x}{k_h}}} \right] \dots\dots\dots (4)$$

Using the short time approximation, we have

$$S(x_D, t_D) = \frac{\beta}{2} \dots\dots\dots (5)$$

Where $\beta = 2$ for $x_D < \sqrt{\frac{k_x}{k}}$; $\beta = 0$ for $x_D > \sqrt{\frac{k_x}{k}}$; and $\beta = 1$ for $x_D = \sqrt{\frac{k_x}{k}}$

Also equation (2) and (3) become

$$S(y_D, t_D) = \frac{1}{2\sqrt{\pi\frac{k_y}{k_h}t_D}} \exp\left[-\frac{(y_D - y_{wD})^2 k_h}{4t_D k}\right] \dots\dots\dots (6)$$

and

$$S(z_D, t_D) = \frac{1}{2\sqrt{\pi t_D \frac{k_z}{k_h}}} \exp\left[-\frac{(z_D - z_{wD})^2 k_z}{4t_D k}\right] \dots\dots\dots (7)$$

Using Newman’s product rule for equations (5), (6) and (7), the final system dimensionless pressure distribution for infinite-acting flow period is

$$P_D(x_D, y_D, z_D, \tau) = \frac{h_D}{4\sqrt{\frac{k k_z}{k_y k_z}}} \int_0^{t_{D1}} \frac{1}{\tau} \left\{ \left[\operatorname{erf} \frac{\sqrt{\frac{k}{k_x} + x_D}}{2\sqrt{\tau}} + \operatorname{erf} \frac{\sqrt{\frac{k}{k_x} - x_D}}{2\sqrt{\tau}} \right] \cdot \left[\exp - \frac{(y_D - y_{wD})^2 \frac{k}{k_y} + (z_D - z_{wD})^2 \frac{k}{k_z}}{4\tau} \right] \right\} d\tau \dots\dots (9)$$

Using the short time approximation for x (from equation (5)), equation (9) become

$$p_{Di} = \frac{-\beta h_D}{4} \sqrt{\frac{k k_z}{k_y k_z}} \left\{ \operatorname{Ei} \left[-\frac{(y_D - y_{wD})^2 \left(\frac{k}{k_y}\right) + (z_D - z_{wD})^2 \frac{k}{k_z}}{4t_D} \right] \right\} \dots\dots\dots (10)$$

Where β is a function representing the short time approximation prior to the time the influences of the x-axis source boundaries are felt.

2.1.2 Early linear flow

If the well length is long in relation to the reservoir thickness and if there is a better vertical permeability than the horizontal permeability, then the flow feels the Z- boundaries first while the y- and x-boundaries are still infinite acting. The required source function is infinite slab source in an infinite reservoir in the X-direction, infinite plane sources for the y- direction and mixed boundaries of infinite plane source for the Z-direction.

X-Axis

$$S(x, t) = \frac{1}{2} \left[\operatorname{erf} \frac{\frac{x_f}{2} + (x - x_w)}{2\sqrt{\eta x t}} + \operatorname{erf} \frac{\frac{x_f}{2} - (x - x_w)}{2\sqrt{\eta x t}} \right] \dots\dots\dots (11)$$

Y-Axis

$$S(y, t) = \exp[-(y - y_w)^2 / 4\eta_y t] / 2\sqrt{\pi\eta_y t} \dots\dots\dots (12)$$

Z-Axis

$$s(z, t) = \frac{2}{z_e} \sum_{m=1}^{\infty} \exp\left(-\frac{(2m-1)^2 \pi^2 \eta_z}{4z_e^2}\right) \sin(2m-1)\pi \frac{z_w}{z_e} \sin(2m-1)\pi \frac{z}{z_e} \dots\dots (13)$$

In dimensionless forms, equations (11) to(13)respectively become:

$$S(x_D, t_D) = \frac{1}{2} \left[\operatorname{erf} \frac{\sqrt{\frac{k}{k_x} + x_D}}{2\sqrt{t_D}} + \operatorname{erf} \frac{\sqrt{\frac{k}{k_x} - x_D}}{2\sqrt{t_D}} \right] \dots\dots\dots (14)$$

$$S(y_D, t_D) = \frac{1}{2\sqrt{\pi t_D}} \exp \frac{-(y_D - y_{wD})^2}{4t_D} \frac{k}{k_y} \dots\dots\dots (15)$$

$$s(z_D, t_D) = \frac{2}{h_D} \sum_{m=1}^{\infty} \exp\left(-\frac{(2m-1)^2 \pi^2 t_D}{4h_D^2}\right) \sin(2m-1)\pi \frac{z_{wD}}{h_D} \sin(2m-1)\pi \frac{z_D}{h_D} \dots\dots (16)$$

Using Newman’s product rule, for equations (14) to (16), we have

$$P_{D1} = \sqrt{\pi} \int_{t_{D1}}^{t_{D2}} \frac{1}{\sqrt{\tau}} \cdot \left[\operatorname{erf} \frac{\sqrt{\frac{k}{k_x} + x_D}}{2\sqrt{\tau}} + \operatorname{erf} \frac{\sqrt{\frac{k}{k_x} - x_D}}{2\sqrt{\tau}} \right] \cdot \exp \frac{-(y_D - y_{wD})^2}{4\tau} \frac{k}{k_y} \cdot \sum_{m=1}^{\infty} \exp\left(-\frac{(2m-1)^2 \pi^2 \tau}{4h_D^2}\right) \sin(2m-1)\pi \frac{z_{wD}}{h_D} \sin(2m-1)\pi \frac{z_D}{h_D} d\tau \dots\dots\dots (17)$$

First steady-state flow period

This period may occur if the wellbore length is short compared with the reservoir thickness and the horizontal permeability is larger than the vertical permeability. If this occurs then flow feels the X-boundaries while the y- and z- boundaries are still infinite acting. The required source function is prescribed pressure for the X-direction and infinite plane sources for the y- and z- direction.

X-Axis:

$$S(x, t) = \frac{4}{\pi} \sum_{n=1}^{\infty} \frac{1}{n} \exp\left(-\frac{n^2 \pi^2 \eta x t}{x_e^2}\right) \sin n \frac{\pi}{2} \cdot \frac{x_f}{x_e} \sin n \pi \frac{x_w}{x_e} \sin n \pi \frac{x}{x_e} \dots\dots\dots (18)$$

Y-Axis

$$S(y,t) = \exp[-(y - y_w)^2/4\eta_y t]/2\sqrt{\pi\eta_y t} \dots\dots\dots (19)$$

Z-Axis

$$S(z,t) = \exp[-(z - z_w)^2/4\eta_z t]/2\sqrt{\pi\eta_z t} \dots\dots\dots (20)$$

In dimensionless forms equations (18) to (20) respectively become

$$S(x_D, t_D) = \frac{4}{\pi} \sum_{n=1}^{\infty} \frac{1}{n} \exp\left(-\frac{(4n^2\pi^2\eta_x)}{x_{eD}^2} \frac{k}{k_h} t_D\right) \sin n \frac{\pi}{2x_{eD}} \sqrt{\frac{k}{k_x}} \sin n\pi \frac{x_{wD}}{x_{eD}} \sin n\pi \frac{x_D}{x_{eD}} \dots\dots\dots (21)$$

$$S(y_D, t_D) = \frac{1}{2\sqrt{\pi t_D}} \frac{k}{k_y} \exp\left(-\frac{(y_D - y_{wD})^2}{4t_D} \frac{k}{k_y}\right) \dots\dots\dots (22)$$

$$S(z_D, t_D) = \frac{1}{2\sqrt{\pi t_D}} \frac{k}{k_z} \exp\left(-\frac{(z_D - z_{wD})^2}{4t_D} \frac{k}{k_z}\right) \dots\dots\dots (23)$$

Using Newman’s product rule for equations (21) to (23), we have

$$P_{D2} = 2h_D \sqrt{\frac{k^2}{k_y k_z}} \int_{t_{D2}}^{t_{D3}} \frac{1}{\tau} \sum_{n=1}^{\infty} \frac{1}{n} \exp\left(-\frac{4n^2\pi^2\tau}{x_{eD}^2}\right) \sin \frac{n\pi}{x_{eD}} \sqrt{\frac{k}{k_x}} \sin \frac{n\pi x_{wD}}{x_{eD}} \sin \frac{n\pi x_D}{x_{eD}} \exp\left(-\frac{r_{wD}^2}{4\tau}\right) d\tau \dots (24)$$

Second steady-state flow period

This period may occur if the wellbore length is long compared to the reservoir thickness. During this flow period, the flow feels the z-boundaries while the x- and y- boundaries are still infinite acting. The required sources functions are an infinite reservoir plane source for the y axis, an infinite slab source for the x-axis and mixed boundaries for an infinite slab source in an infinite slab reservoir for the z-axis. The required source functions are:

X-Axis

$$S(x,t) = \frac{1}{2} \left[\operatorname{erf} \frac{\frac{x_f}{2} + (x - x_w)}{2\sqrt{\eta_x t}} + \operatorname{erf} \frac{\frac{x_f}{2} - (x - x_w)}{2\sqrt{\eta_x t}} \right] \dots\dots\dots (25)$$

Y-Axis

$$S(y,t) = \exp[-(y - y_w)^2/4\eta_y t]/2\sqrt{\pi\eta_y t} \dots\dots\dots (26)$$

Z-Axis

$$S(z,t) = \frac{2}{z_e} \sum_{m=1}^{\infty} \exp\left(-\frac{(2m-1)^2\pi^2\eta_z}{4z_e^2}\right) \sin(2m-1)\pi \frac{z_w}{z_e} \sin(2m-1)\pi \frac{z}{z_e} \dots\dots\dots (27)$$

In dimensionless forms, equations (25) to (27) respectively become:

$$S(x_D, t_D) = \frac{1}{2} \left[\operatorname{erf} \sqrt{\frac{k}{k_x}} \frac{\frac{x_D}{2} + x_D}{2\sqrt{t_D}} + \operatorname{erf} \sqrt{\frac{k}{k_x}} \frac{\frac{x_D}{2} - x_D}{2\sqrt{t_D}} \right] \dots\dots\dots (28)$$

$$S(y_D, t_D) = \frac{1}{2\sqrt{\pi t_D}} \exp\left(-\frac{(y_D - y_{wD})^2}{4t_D} \frac{k}{k_y}\right) \dots\dots\dots (29)$$

$$s(z_D, t_D) = \frac{2}{h_D} \sum_{m=1}^{\infty} \exp\left(-\frac{(2m-1)^2\pi^2 t_D}{4h_D^2}\right) \sin(2m-1)\pi \frac{z_{wD}}{h_D} \sin(2m-1)\pi \frac{z_D}{h_D} \dots\dots\dots (30)$$

$$p_{D3} = \sqrt{\pi} \int_{t_{D3}}^{t_{D4}} \frac{1}{\sqrt{\tau}} \left[\operatorname{erf} \sqrt{\frac{k}{k_x}} \frac{\frac{x_D}{2} + x_D}{2\sqrt{\tau}} + \operatorname{erf} \sqrt{\frac{k}{k_x}} \frac{\frac{x_D}{2} - x_D}{2\sqrt{\tau}} \right] \left[\exp\left(-\frac{(y_D - y_{wD})^2}{4\tau} \frac{k}{k_y}\right) \cdot \left[\sum_{m=1}^{\infty} \exp\left(-\frac{(2m-1)^2\pi^2\tau}{4h_D^2}\right) \sin(2m-1)\pi \frac{z_{wD}}{h_D} \sin(2m-1)\pi \frac{z_D}{h_D} \right] d\tau \dots\dots\dots (31)$$

Late steady-state flow period

The flow feels the X- and Z- boundaries while the y- boundary is still infinite acting. The required source function is prescribed pressure in the X-direction, mixed boundaries for infinite plane source for the Z-direction and infinite plane sources for the y- direction.

X-Axis

$$S(x,t) = \frac{4}{\pi} \sum_{n=1}^{\infty} \frac{1}{n} \exp\left(-\frac{n^2\pi^2\eta_x t}{x_e^2}\right) \sin n \frac{\pi}{2} \frac{x_f}{x_e} \sin n\pi \frac{x_w}{x_e} \sin n\pi \frac{x}{x_e} \dots\dots\dots (32)$$

Y-Axis

$$S(y,t) = \exp[-(y - y_w)^2/4\eta_y t]/2\sqrt{\pi\eta_y t} \dots\dots\dots (33)$$

Z-Axis

$$S(z,t) = \frac{2}{z_e} \sum_{m=1}^{\infty} \exp\left(-\frac{(2m-1)^2\pi^2\eta_z}{4z_e^2}\right) \sin(2m-1)\pi \frac{z_w}{z_e} \sin(2m-1)\pi \frac{z}{z_e} \dots\dots\dots (34)$$

In dimensionless forms equations (32), (33) and (34) respectively become

$$S(x_D, t_D) = \frac{4}{\pi} \sum_{n=1}^{\infty} \frac{1}{n} \exp\left(-\frac{(4n^2\pi^2)}{x_{eD}^2} \frac{k}{k_h} t_D\right) \sin n \frac{\pi}{2x_{eD}} \sqrt{\frac{k}{k_x}} \sin n\pi \frac{x_{wD}}{x_{eD}} \sin n\pi \frac{x_D}{x_{eD}} \dots\dots\dots (35)$$

$$S(y_D, t_D) = \frac{1}{2\sqrt{\pi t_D}} \frac{k}{k_y} \exp\left(-\frac{(y_D - y_{wD})^2}{4t_D} \frac{k}{k_y}\right) \dots\dots\dots (36)$$

And

$$s(z_D, t_D) = \frac{2}{h_D} \sum_{m=1}^{\infty} \exp\left(-\frac{(2m-1)^2 \pi^2 t_D}{4h_D^2}\right) \sin(2m-1)\pi \frac{z_{WD}}{h_D} \sin(2m-1)\pi \frac{z_D}{h_D} \dots \quad (37)$$

Using Newman’s product rule for equations (35) to (37), we have

$$p_{D4} = \frac{8}{\sqrt{\pi}} \int_{t_{D4}}^{t_{D5}} \frac{1}{\sqrt{\tau}} \sum_{n=1}^{\infty} \sum_{m=1}^{\infty} \frac{1}{n} \exp\left(-\frac{(4n^2 \pi^2)}{x_{eD}^2} \tau \frac{k}{k_h}\right) \sin n \frac{\pi}{2x_{eD}} \sqrt{\frac{k}{k_x}} \sin n \pi \frac{x_{WD}}{x_{eD}} \sin n \pi \frac{x_D}{x_{eD}} \cdot \exp\left(-\frac{(2m-1)^2 \pi^2 \tau}{4h_D^2}\right) \sin(2m-1)\pi \frac{z_{WD}}{h_D} \sin(2m-1)\pi \frac{z_D}{h_D} \exp\left(-\frac{(y_D-y_{WD})^2}{4\tau} \frac{k}{k_y}\right) d\tau \dots \quad (38)$$

Using superposition principle, we have

$$p_D = p_{Di} + p_{D1} + p_{D2} + p_{D3} + p_{D4} \dots \quad (39)$$

2.2 Solution to Flow Equations

Putting equations (10), (17), (24),(31) and (38) into equation(39) gives

$$p_D = \frac{-\beta h_D}{4} \sqrt{\frac{k k}{k_y k_z}} \left\{ Ei \left[-\frac{r_{WD}^2 k}{4t_D} \right] \right\} + \sqrt{\pi} \int_{t_{D1}}^{t_{D2}} \frac{1}{\sqrt{\tau}} \cdot [erf \sqrt{\frac{k}{k_x} + x_D} + erf \sqrt{\frac{k}{k_x} - x_D}] \cdot \exp\left(-\frac{(y_D-y_{WD})^2}{4\tau} \frac{k}{k_y}\right) \cdot \sum_{m=1}^{\infty} \exp\left(-\frac{(2m-1)^2 \pi^2 \tau}{4h_D^2}\right) \sin(2m-1)\pi \frac{z_{WD}}{h_D} \sin(2m-1)\pi \frac{z_D}{h_D} d\tau + 2h_D \sqrt{\frac{k^2}{k_y k_z}} \int_{t_{D2}}^{t_{D3}} \frac{1}{\tau} \cdot \sum_{n=1}^{\infty} \frac{1}{n} \exp\left(-\frac{4n^2 \pi^2 \tau}{x_{eD}^2}\right) \sin \frac{n\pi}{x_{eD}} \sqrt{\frac{k}{k_x}} \cdot \sin \frac{n\pi x_{WD}}{x_{eD}} \cdot \sin \frac{n\pi x_D}{x_{eD}} \cdot \exp\left(-\frac{r_{WD}^2}{4\tau}\right) d\tau + \sqrt{\pi} \int_{t_{D3}}^{t_{D4}} \frac{1}{\sqrt{\tau}} \left[erf \sqrt{\frac{k}{k_x} + x_D} + erf \sqrt{\frac{k}{k_x} - x_D} \right] \left[\exp\left(-\frac{(y_D-y_{WD})^2}{4\tau} \frac{k}{k_y}\right) \cdot \left[\sum_{m=1}^{\infty} \exp\left(-\frac{(2m-1)^2 \pi^2 \tau}{4h_D^2}\right) \sin(2m-1)\pi \frac{z_{WD}}{h_D} \sin(2m-1)\pi \frac{z_D}{h_D} \right] d\tau + \frac{8}{\sqrt{\pi}} \int_{t_{D4}}^{t_{D5}} \frac{1}{\sqrt{\tau}} \left[\sum_{n=1}^{\infty} \frac{1}{n} \exp\left(-\frac{(4n^2 \pi^2)}{x_{eD}^2} \tau \frac{k}{k_h}\right) \sin n \frac{\pi}{2x_{eD}} \sqrt{\frac{k}{k_x}} \sin n \pi \frac{x_{WD}}{x_{eD}} \sin n \pi \frac{x_D}{x_{eD}} \right] \cdot \left[\exp\left(-\frac{(y_D-y_{WD})^2}{4\tau} \frac{k}{k_y}\right) \cdot \left[\sum_{m=1}^{\infty} \exp\left(-\frac{(2m-1)^2 \pi^2 \tau}{4h_D^2}\right) \sin(2m-1)\pi \frac{z_{WD}}{h_D} \sin(2m-1)\pi \frac{z_D}{h_D} \right] d\tau \dots \quad (40)$$

Assumed field data:

L=1000ft, X_w=400ft, X_e=1250ft, X= 610ft, y=300ft, y_e=1200ft, Z_w=49.9137ft, y_w=390ft, Z=50ft, and h=704ft, k_x=10, k_y=0.025, k_z=2

3.0 Result and Discussion

Dimensionless pressure was computed for equations (10), and (40). Results of our numerical computation are shown in Tables 1 to 6 and plotted in Figures 2 to 7.

Table 1: T_D VERSUS P_D ACCORDING TO EQUATION (10), FOR L_D=0.5 AND R_{WD} = 1E-4, 1E-5 AND 1E-6

TD	PD(LD=0.5, RWD=1E-4)	PD(LD=0.5, RWD=1E5)	PD(LD=0.5, RWD=1E-6)
1.0E-05	27.3913	43.7375	60.0838
1.0E-04	35.5644	51.9107	68.2569
1.0E-03	43.7375	60.0838	76.4300
1.0E-02	51.9107	68.2569	84.6031
0.1	60.0838	76.4300	92.7762
1.0	68.2569	84.6031	100.949
10.0	76.4300	92.7762	109.122
100.0	84.6031	100.949	117.296
1000.0	92.7762	109.122	125.469
10000.0	100.949	117.296	133.642
100000.	109.122	125.469	141.815

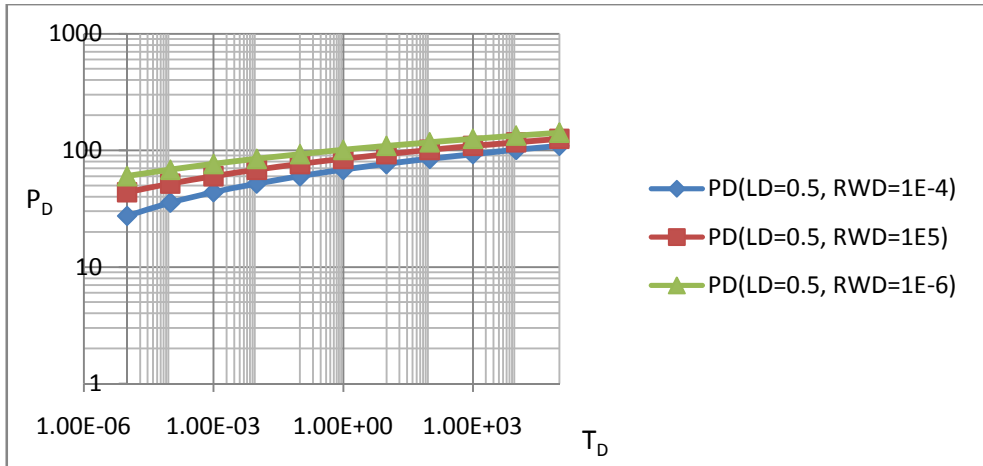


FIG. 2: T_D VERSEUS P_D ACCORDING TO EQUATION (10), FOR $L_D=0.5$ AND $R_{WD} = 1E-4, 1E-5$ AND $1E-6$

TABLE 2: T_D VERSEUS P_D ACCORDING TO EQUATION (10), FOR $L_D=1$ AND $R_{WD} = 1E-4, 1E-5$ AND $1E-6$

TD	PD(LD=1, RWD=1E-4)	PD(LD=1, RWD=1E-5)	PD(LD=1, RWD=1E-6)
1.0E-05	13.6957	21.8688	30.0419
1.0E-04	17.7822	25.9553	34.1284
1.0E-03	21.8688	30.0419	38.2150
1.0E-02	25.9553	34.1284	42.3015
0.1	30.0419	38.2150	46.3881
1.0	34.1284	42.3015	50.4747
10.0	38.2150	46.3881	54.5612
100.0	42.3015	50.4747	58.6478
1000.0	46.3881	54.5612	62.7343
10000.0	50.4747	58.6478	66.8209
100000.	54.5612	62.7343	70.9074

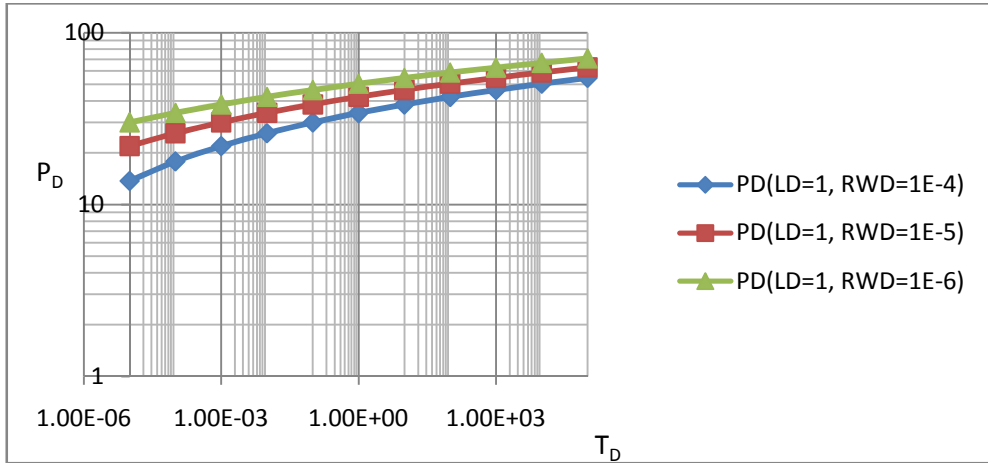


FIG. 3: T_D VERSEUS P_D ACCORDING TO EQUATION (10), FOR $L_D=1$ AND $R_{WD} = 1E-4, 1E-5$ AND $1E-6$

TABLE 3: T_D VERSEUS P_D ACCORDING TO EQUATION (10), FOR $L_D=2.5$ AND $R_{WD} = 1E-4, 1E-5$ AND $1E-6$

TD	PD(LD=2-5, RWD=1E-4)	PD(LD=2-5, RWD=1E-5)	PD(LD=2-5, RWD=1E-6)
1.0E-05	5.47827	8.74751	12.0168
1.0E-04	7.11289	10.3821	13.6514
1.0E-03	8.74751	12.0168	15.2860
1.0E-02	10.3821	13.6514	16.9206
0.1	12.0168	15.2860	18.5552
1.0	13.6514	16.9206	20.1899
10.0	15.2860	18.5552	21.8245
100.0	16.9206	20.1899	23.4591
1000.0	18.5552	21.8245	25.0937
10000.0	20.1899	23.4591	26.7284
100000.	21.8245	25.0937	28.3630

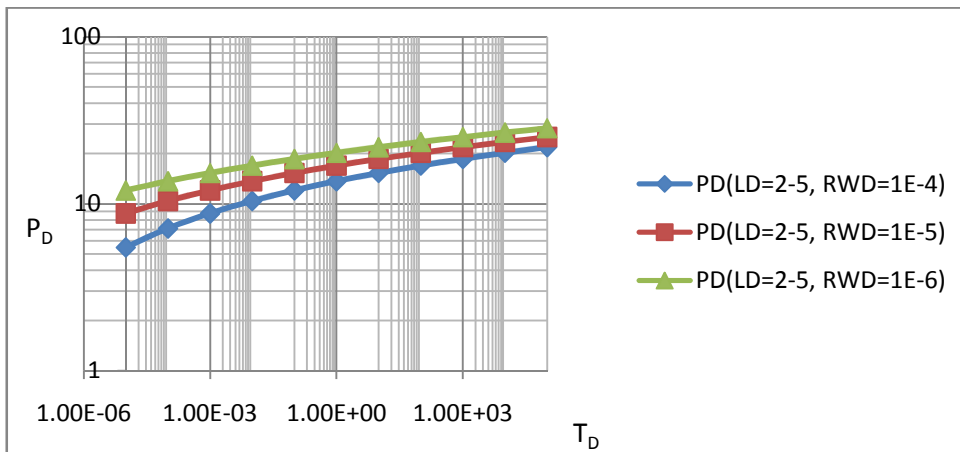


FIG. 4: T_D VERSEUS P_D ACCORDING TO EQUATION (10), FOR $L_D=2.5$ AND $R_{WD} = 1E-4, 1E-5$ AND $1E-6$

TABLE 4: T_D VERSEUS P_D ACCORDING TO EQUATION (40), FOR $L_D=0.5$ AND $R_{WD} = 1E-4, 1E-5$ AND $1E-6$

TD	PD(LD=0.5, RWD=1E-4)	PD(LD=0.5, RWD=1E5)	PD(LD=0.5, RWD=1E-6)
1.0E-05	27.3913	43.7375	60.0838
1.0E-04	35.5644	51.9107	68.2569
1.0E-03	43.7375	60.0838	76.4300
1.0E-02	51.9107	68.2569	84.6031
0.1	60.0838	76.4300	92.7762
1.0	68.2569	84.6031	100.949
10.0	76.4300	92.7762	109.122
100.0	84.6031	100.949	117.296
1000.0	84.6031	100.949	117.296
10000.0	84.6031	100.949	117.296
100000.	84.6031	100.949	117.296

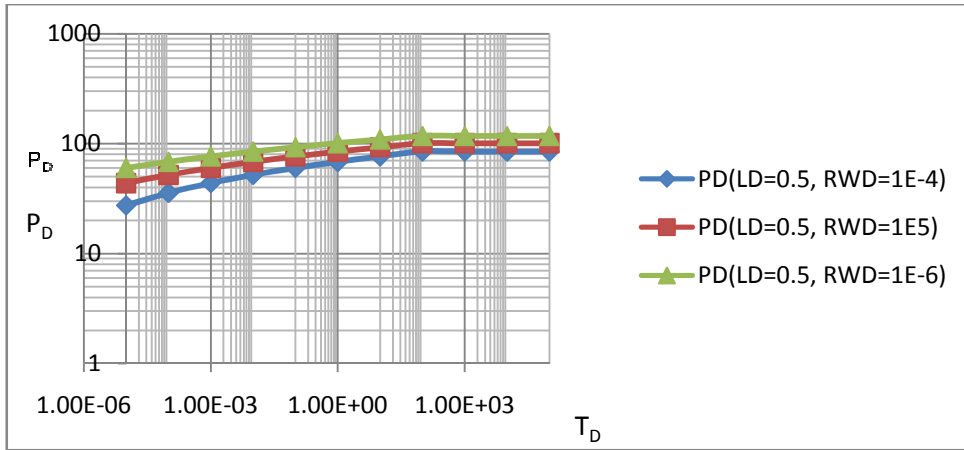


FIG. 5: T_D VERSEUS P_D ACCORDING TO EQUATION (40), FOR $L_D=0.5$ AND $R_{WD} = 1E-4, 1E-5$ AND $1E-6$

TABLE 5: T_D VERSEUS P_D ACCORDING TO EQUATION (40), FOR $L_D=1.0$ AND $R_{WD} = 1E-4, 1E-5$ AND $1E-6$

TD	PD(LD=1, RWD=1E-4)	PD(LD=1, RWD=1E-5)	PD(LD=1, RWD=1E-6)
1.0E-05	13.6957	21.8688	30.0419
1.0E-04	17.7822	25.9553	34.1284
1.0E-03	21.8688	30.0419	38.2150
1.0E-02	25.9553	34.1284	42.3015
0.1	30.0419	38.2150	46.3881
1.0	34.1284	42.3015	50.4747
10.0	38.2150	46.3881	54.5612
100.0	42.3015	50.4747	58.6478
1000.0	42.3015	50.4747	58.6478
10000.0	42.3015	50.4747	58.6478
100000.	42.3015	50.4747	58.6478

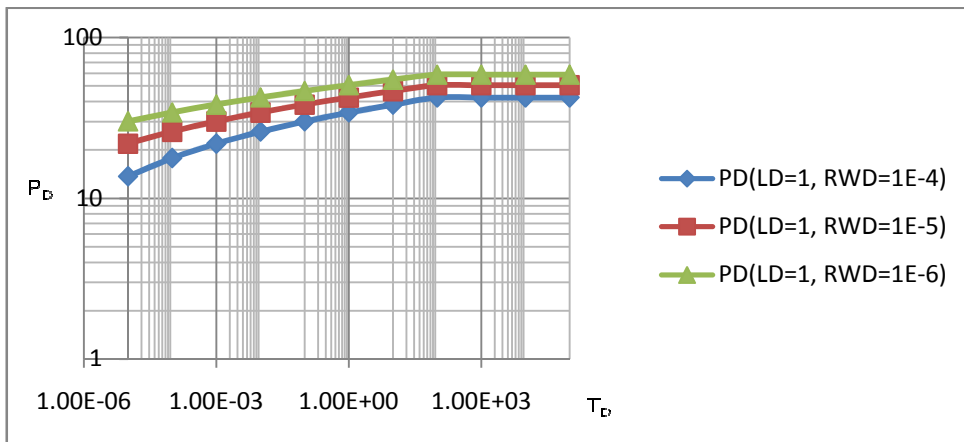
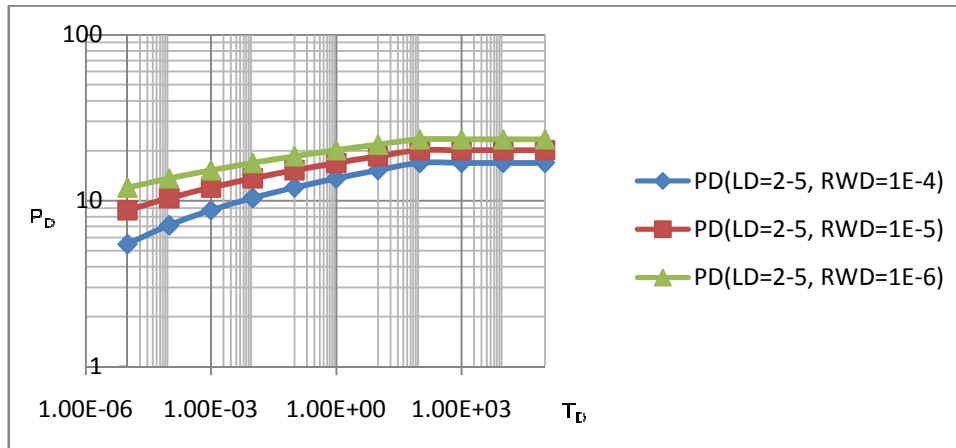


FIG. 6: T_D VERSEUS P_D ACCORDING TO EQUATION (40), FOR $L_D=1.0$ AND $R_{WD} = 1E-4, 1E-5$ AND $1E-6$

TABLE 6: T_D VERSUS P_D ACCORDING TO EQUATION (40), FOR $L_D=2.5$ AND $R_{WD} = 1E-4, 1E-5$ AND $1E-6$

T_D	PD(LD=2-5, RWD=1E-4)	PD(LD=2-5, RWD=1E-5)	PD(LD=2-5, RWD=1E-6)
1.0E-05	5.47827	8.74751	12.0168
1.0E-04	7.11289	10.3821	13.6514
1.0E-03	8.74751	12.0168	15.2860
1.0E-02	10.3821	13.6514	16.9206
0.1	12.0168	15.2860	18.5552
1.0	13.6514	16.9206	20.1899
10.0	15.2860	18.5552	21.8245
100.0	16.9206	20.1899	23.4591
1000.0	16.9206	20.1899	23.4591
10000.0	16.9206	20.1899	23.4591
100000.	16.9206	20.1899	23.4591

FIG. 7: T_D VERSUS P_D ACCORDING TO EQUATION (40), FOR $L_D=2.5$ AND $R_{WD} = 1E-4, 1E-5$ AND $1E-6$

4.0 Conclusion

The study showed how permeability ratio, wellbore radius and reservoir height can affect the production of oil and gas from a horizontal well which experiences simultaneous two edged and bottom water drive mechanism.

Dimensionless pressure for horizontal well centrally located in the reservoir subject to edge water were formulated and computed. The reservoir is later

Influenced by an aquifer which affects it from the edge and bottom. Results show that:

- (i) At higher values of r_{wD} , higher pressures are observed. This indicates that as we move deeper into the reservoir, the aquifer support becomes more pronounced.
- (ii) The smaller the well length ($l_D=1/h_D$), the higher the pressure for the same wellbore radius.
- (iii) The smaller the wellbore radius the higher the pressure for the same well length.
- (iv) The rate of pressure increase with time is higher for the infinite period than any other flow regime.
- (v) Rate of pressure increase is higher in reservoir with horizontal permeability than reservoir with vertical permeability.

References:

- [1]. Goode, P.A. and Thambynayagam, R.K.M.: "Pressure Drawdown and Buildup Analysis for Horizontal Well in Anisotropic Media," SPEFE(Dec.1987)683-697, Trans., AIME, 283.
- [2]. Odeh, A.S. and Babu, O.K.: "Transient Flow Behavior of Horizontal Wells: Pressure Drawdown and Buildup Analysis," SPEFE (March 1990) 7; Trans., AIME, 289
- [3]. E. S. Adewole and K. O. Bello: "Pressure Transient Analysis in a Horizontal Well subject to four Vertical wells injector". Journal of Nigeria Association of Mathematical Physics. Vol. 8, (Nov. 2004), pp 75 – 82
- [4]. E. S. Adewole: "Pressure Gradient and Pressure Derivatives Characteristics of a Horizontal Well Subject to Bottom Water Drive" Journal of the Nigerian Association of Mathematical Physics Vol. 12 (May 2008) pp 225 – 236.

- [5] E. S. Adewole: “*The Use of Sources and Green’s function to Model Pressure Distribution in a bounded Reservoir with Lateral Wells. Part II: General Solution*”*Journal of the Nigerian Association of Mathematical Physics* vol. 15 (Nov. 2009), pp 197 – 204
- [6]. Karakas, M Yokoyama, Y.M. and Arima, E. M. : “Well Test Analysis of a Well with Multiple Horizontal Drainholes”, SPE21424 presented at the Middle East Oil Show, Bahrain, November 16-19, 1991.
- [7]. Raghavan, R. and Ambashta, A.K. : “An Assessment of Productivity of Multilateral Completions” *Journal of Canadian Petroleum Technology* (October 1998) 58.
- [8]. Gringarten, A., and Ramey, H. J., 1973, “*The Use of Source and Green’s Function’s in solving Unsteady-Flow Problems in Reservoirs,*” *SPE Journal*, October, 1973, 285-296.
- [9]. Cinco-Ley H., Miller F. G. and Ramey H. J. (Jr): “Unsteady-State Pressure Distribution Created by a Directionally Drilled Wells” *JPT*(Nov.1975) 1392-1400.
- [10]. Raghavan R., Uraiet,A. and Thomas G. W : “Vertical Fracture Height: Effects on Transient Flow Behaviour” paper SPE 6061 presented on the 51stAnnual Conference and Exhibition, New Orleans, Oct 3-6 1976.
- [11]. Rodriguez, F.et al.: “Partially Penetrating Fractures; Pressure Transient Analysis of an Infinite Conductivity Fracture” paper SPE 12743 presented at the 1984 SPE California Regional Meeting, Long Beach, April 11-13.